LTV ASTRONAUTICS DIVISION
LTV AEROSPACE CORPORATION
P.O. BOX 6267 DALLAS, TEXAS 75222

AMU TRAINING SIMULATION PROGRAM

REPORT NO. 00.794

27 APRIL 1966

CONTRACT NO. NAS9-5711

Prepared By:

H.E. Sewell, Jr.
Technical Project Engineer
Manned Aerospace Flight Simulator

Approved By:

M.H. Bradshaw
Manager
Laboratories

Reviewed By:

W.J. North, Jr.
Supervisor
Manned Aerospace Flight Simulator

C.H. Coleman
Manager
Research Administration

NASA CR 92163

SUMMARY

A simulation program in the LTV Astronautics Manned Aerospace Flight Simulator (MAFS) was used to provide training of the GT-9 primary and backup pilots, Cernan and Aldrin, in the operation and handling qualities of the LTV Astronaut Maneuvering Unit (AMU). The simulation program was operated for a period of two weeks, including the NASA engineering review phases, with a total of over 100 simulated runs being performed. The training runs for the two astronauts, a total of 51 varying in length from as little as about 10 minutes to as much as 75 minutes, were performed in a four day period, 28 through 31 March 1966.

The program involved the performance of various maneuvers with the AMU rotations and translations relative to both simulated Gemini and Agena spacecraft. Control of the AMU was evaluated in both the automatic and manual attitude modes and with various failure modes. Several guidance techniques for effecting transfers, translations, to the spacecraft were investigated. A technique for the gross transfer maneuver which involved establishing a closure rate and then yawing the AMU such that the thruster alignment relative to the line-of-sight provided two-dimensional translational control of line-of-sight rotation proved to be most promising.

The simulation utilized the MAFS moving base simulator and a hybrid, digital-analog computer arrangement. The MAFS cockpit incorporated an actual AMU backpack structure with controller arms, a simulated chest pack, and a suit pressurization system. Visual displays included a horizon projector for AMU attitude relative to the Earth and a two-spot projector, the spots representing the two ends of the simulated spacecraft, Gemini or Agena. The computer provided real time simulation of the AMU in six-degrees-of-freedom, the selected spacecraft in three degrees-of-freedom. Interfaced between the AMU controls in the MAFS cockpit and the computer was a control box which contained an actual AMU control electronics package and provisions for inserting thruster and gyro failures. Inputs to the box included the simulated rate gyro signals and AMU control signals to the control electronics, the outputs being the individual thruster on-off commands to the computer.

TABLE OF CONTENTS

1.0	INTRODUCTION	1
2.0	OPERATIONAL PROCEDURE AND RESULTS	2
3.0	CONCLUSIONS AND RECOMMENDATIONS	8
4.0	SIMULATOR MECHANIZATION	9
4.1	DESCRIPTION OF FACILITY	9
4.2	EQUATIONS AND TECHNICAL DESCRIPTION	15
4.3	DATA RECORDING	36
4.4	VEHICLE CONFIGURATION AND INITIAL CONDITION DATA	37

FIGURES

2.0-1	Astronaut Aldrin in MAFS-AMU Simulator	3
2.0-2	Astronaut Aldrin in MAFS-AMU Simulator with Pressure Suit	4
2.0-3	Astronaut Cernan in MAFS-AMU Simulator	5
2.0-4	Astronaut Cernan in MAFS-AMU Simulator with Pressure Suit	6
4.1-1	AMU Simulator Equipment Block Diagram	10
4.1-2	AMU Control Electronics and Failure Logic Box	12
4.1-3	AMU Simulation - Master Control Station	13
4.2-1	AMU Simulation - Translation Geometry	16
4.2-2	AMU Geometry	17
4.2-3	Line-of-Sight Coordinate System	20
4.2-4	Euler Angle Geometry	23
4.2-5	Gemini/Agena Spacecraft Geometry	26
4.2-6	Target Projector Geometry	28

1.0 INTRODUCTION

A real time, six degrees-of-freedom simulation of the LTV Astronaut Maneuvering Unit (AMU) was performed to provide training for the GT-9 primary and backup pilots who will conduct the first space operation with the AMU. The basic objectives of this program were the development of both optimum AMU flight procedures and astronaut proficiency in maneuvering with the AMU.

The simulation was conducted at LTV Aerospace Corporation in Dallas, Texas, using the LTV Astronautics Division Manned Aerospace Flight Simulator (MAFS) and LTV simulation and hybrid computations facilities. Simulator operations, which covered a two week period, involved both astronaut training and NASA engineering review phases. The GT-9 primary and backup AMU pilots, Astronauts Cernan and Aldrin, respectively, each received two days of training in the simulator. The engineering phase of the simulation was conducted primarily by two NASA-MSC engineers and one Air Force officer, a pilot assigned to the AMU program. Each of the subject pilots was familiarized with the translational and rotational handling qualities of the AMU and with the effects of various failure modes. Transfer to and docking with both simulated Gemini and Agena spacecraft were evaluated using several guidance techniques.

The primary purpose of this report is to describe the simulation set-up and its mechanization. Prior to this discussion, the report presents a brief description of the operational procedures and results of the simulation along with the resultant conclusions and recommendations for future AMU training simulations as qualitatively observed by LTV personnel.

2.0 OPERATIONAL PROCEDURE AND RESULTS

Two basic types of simulator test flights were made during the astronaut training phase of the program. For each, the AMU was started from a position in front of, on the longitudinal axis, and facing the selected target spacecraft. Each run was conducted under simulated daylight conditions, the visual display system projecting only an earth scene of cloud coverage over the ocean, with no stars being visible. The Gemini was oriented with the longitudinal axis normal to its orbital plane, facing orbital north - orbital east being the direction of orbital motion. The Agena was oriented normal to its orbital plane and facing orbital south. Those runs which started in front of the Gemini were primarily used for initial familiarization with the simulation set-up and AMU handling qualities. Included in these tests were the rotational (yaw, pitch, and roll) and translational (forward, aft, up, and down) maneuvers which will form the initial maneuvering checks of the AMU to be performed on the GT-9 flight. Also included were translations from a distance of about 10 feet to ranges up to about 125 feet from which transfer back to and docking with the Gemini were practiced. The tests with the simulated Agena basically involved the out-of-plane transfer maneuver from the vicinity of the Gemini to the nose of the Agena, a distance of 80 feet, followed by a translation out from the side of the Agena, approximately in-plane, to a range of about 80 feet. From that position transfer back to the Agena with simulated docking was then performed.

The actual procedures used and lengths of the simulation runs were quite variable, the choice being primarily that of the individual astronaut. Run length varied from as little as about 10 minutes to as much as 75 minutes. Each of the astronauts received his initial simulator familiarization runs under "shirt sleeve" conditions but the major portion of his training, starting the afternoon of the first day, was attained while wearing his pressure suit and pressurized to a differential of 3.7 psi. Photographs of each of the astronauts in the simulator in both "shirt sleeve" and pressure suit conditions are presented as Figures 2.0-1, 2.0-2, 2.0-3, and 2.0-4.

Two basic guidance techniques were evaluated and practiced by the astronauts for effecting a line-of-sight transfer to the spacecraft. Both techniques resulted from the thruster configuration of the AMU - i.e., the ability to translate in only two dimensions, fore-aft and up-down. For the first method the AMU is oriented such that the fore-aft thrusters are aligned with the line-of-sight to the spacecraft, the pilot facing the spacecraft, with roll about the line-of-sight being used to align the up-down thrusters in the plane of rotation of the line-of-sight. For the other method, referred to as "over-the-shoulder" and which proved to be most promising, the AMU was initially oriented facing the spacecraft to establish a closure rate. Then the AMU was yawed about 90 degrees, with subsequent rotations as required, to align both the fore-aft and up-down thrusters normal to the line-of-sight, providing two dimensional translational control for line-of-sight rotations. This alignment could be maintained for the entire transfer up to contact with the spacecraft providing the rate of closure was not excessive, in which case the AMU would have to be yawed to align the fore-aft thrusters with the direction of motion to perform a terminal braking maneuver.

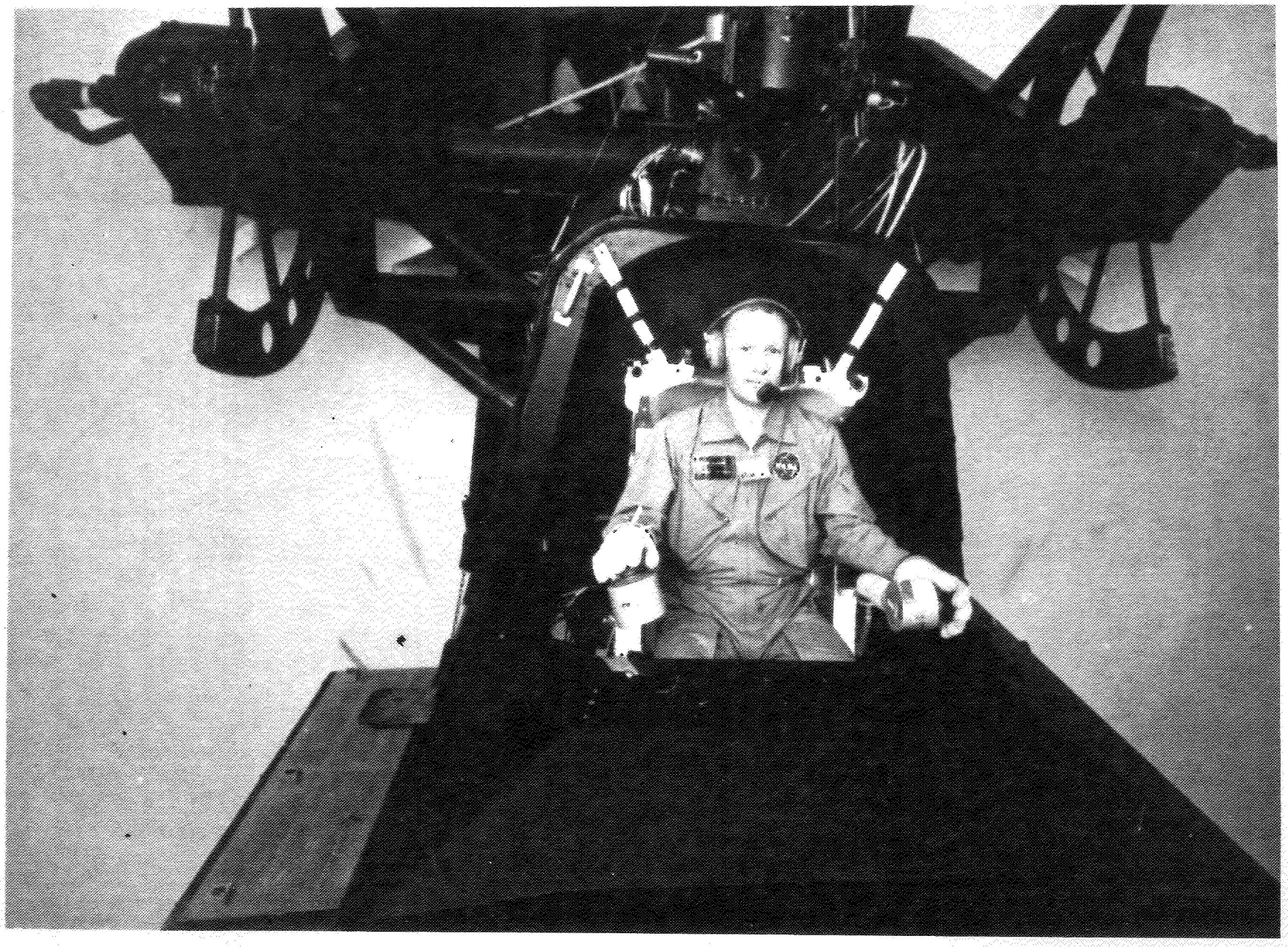

FIG. 2.0-1 ASTRONAUT ALDRIN IN MAFS-AMU SIMULATOR

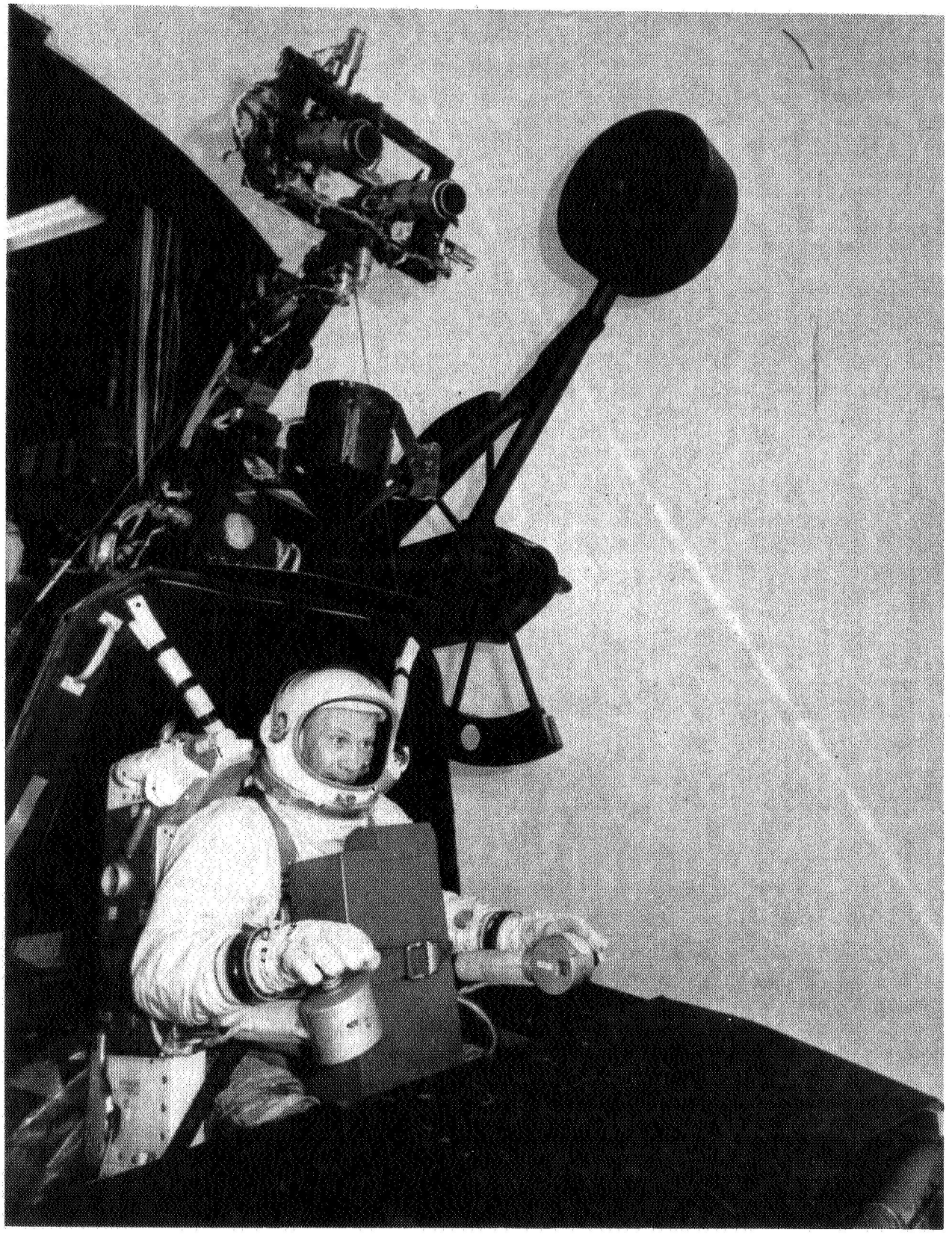

FIG. 2.0-2 ASTRONAUT ALDRIN IN MAFS-AMU SIMULATOR WITH PRESSURE SUIT

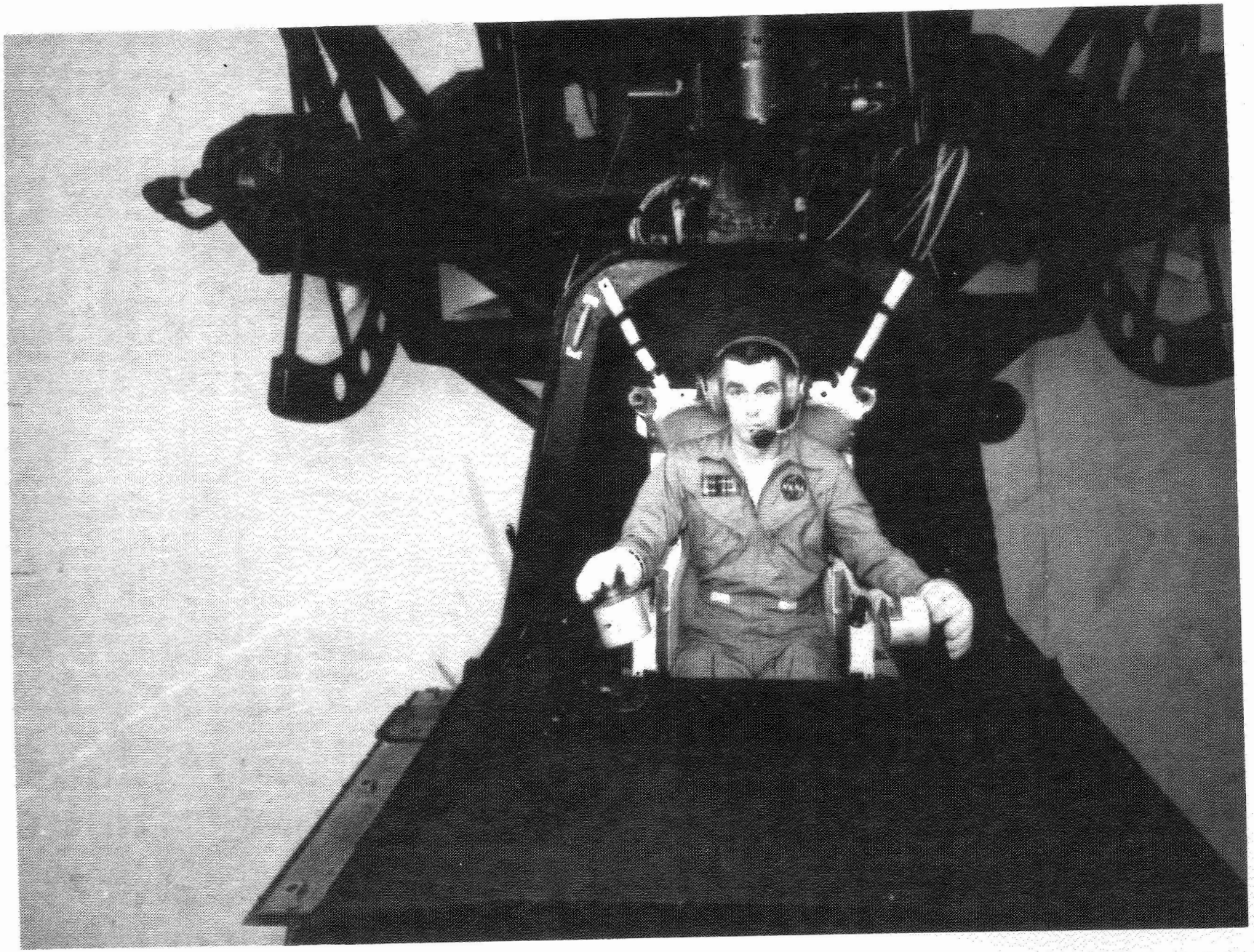

FIG. 2.0-3 ASTRONAUT CERNAN IN MAFS-AMU SIMULATOR

FIG. 2.0-4 ASTRONAUT CERNAN IN MAFS-AMU SIMULATOR WITH PRESSURE SUIT

With the failure logic provisions of the simulation, the astronauts were familiarized with the effects of individual thruster and gyro failures (both on and off) and with fuel (nitrogen supply) pressure failures.

Line printer data were obtained for each of the astronaut runs, with records of the X-Y relative range plots being made on selected runs. The relative range plotters (R_{XT} vs. R_{ZT}, R_{YT} vs. R_{ZT}, and R_{XT} vs. R_{YT}) and the range-range rate ($\dot{\rho}$ vs. ρ) and cross range velocity (V_E vs. V_B) plotter were utilized on every run as real time displays for providing information as required to facilitate the astronaut training.

3.0 CONCLUSIONS AND RECOMMENDATIONS

From observations of the AMU training program by LTV personnel and the comments received from the two astronauts, it is concluded that the subject simulation was a very useful training aid for the initial AMU mission on GT-9. The simulation provided a realistic presentation of the AMU performance and handling qualities, both under normal operation and with the effects of various failure modes. The "over-the-shoulder" guidance technique, which was possible to evaluate with the visual display capabilities of the LTV simulator, was shown to have excellent qualities in relation to ease and accuracy of line-of-sight control.

Although the lack of specific training procedures was justifiable for this program, it is recommended that future training programs of this type have more definite plans of action. They should be based on the experience gained from the GT-9 mission in combination with the recommendations of the astronauts and astronaut training personnel and they should include compliance with procedures for the intended mission. The major portion of the training for each of the astronauts, primary and backup, should follow identical program plans with only a minor part being relegated to basic familiarization.

4.0 SIMULATOR MECHANIZATION

4.1 DESCRIPTION OF FACILITY

The subject simulation utilized the LTV Manned Aerospace Flight Simulator (MAFS) in conjunction with a hybrid computer facility. A block diagram of the simulation equipment is presented as Figure 4.1-1.

4.1.1 Moving Base Simulator

Views of the astronauts in the simulator gondola are shown in Figures 2.0-1 through 2.0-4. The gondola is mounted on a four-gimballed moving base inside a 20 foot diameter spherical projection screen. The motion capabilities of the moving base are ±10 degrees in yaw and inner pitch, ±20 degrees in roll, and ±100 degrees in outer pitch. The yaw and inner pitch motions, because of the 6 foot arm which exists between their pivot point and the pilot station, are used to provide both angular and translational acceleration cues -- yaw and lateral and pitch and normal, respectively. The roll motion provides the roll angular acceleration cue. The outer pitch is normally used to provide the longitudinal acceleration cue but was not used for this program since it lacks the response capabilities for following the low-level pulsating thrusts of the AMU.

4.1.2 AMU Controls and Displays

Incorporated in the gondola cockpit for this program was a production AMU backpack. Functional AMU controls were the rotational and translational controllers, the attitude mode select switch, and the primary and alternate RCS control switches. For the simulation the RCS switches were so configured as to require the primary switch to always be in the on position to supply control electrical power, the function of the alternate switch being to override simulated thruster and gyro failures. A simulated, dummy, chestpack was used which had the fuel remaining gage and three warning light (30% fuel remaining, RCS failure, and fuel pressure failure) displays along with a switch for disabling the abort alarm.

4.1.3 Visual Displays

Two point-source light projection systems, as can be seen in Figures 2.0-2 and 2.0-4, were used to project the visual displays on the MAFS spherical screen. A four-gimballed horizon projector having full rotation capabilities displayed AMU orientation with relation to the Earth horizon and a scene of cloud coverage over an ocean. AMU orientation and position relative to the two ends of the Gemini or Agena spacecraft were displayed by two circular spots of light, blue and red to represent the nose and aft ends, respectively. The spot projector consists of two projection tubes for varying spot diameter with line-of-sight range mounted in a four-gimballed yoke to provide azimuth and elevation deflections of each spot. This arrangement is such that both spots were driven by the azimuth and elevation of the line-of-sight to the nose (blue) end with the red (aft end) spot being driven, in addition, by the differential azimuth and elevation between the lines-of-sight to both ends.

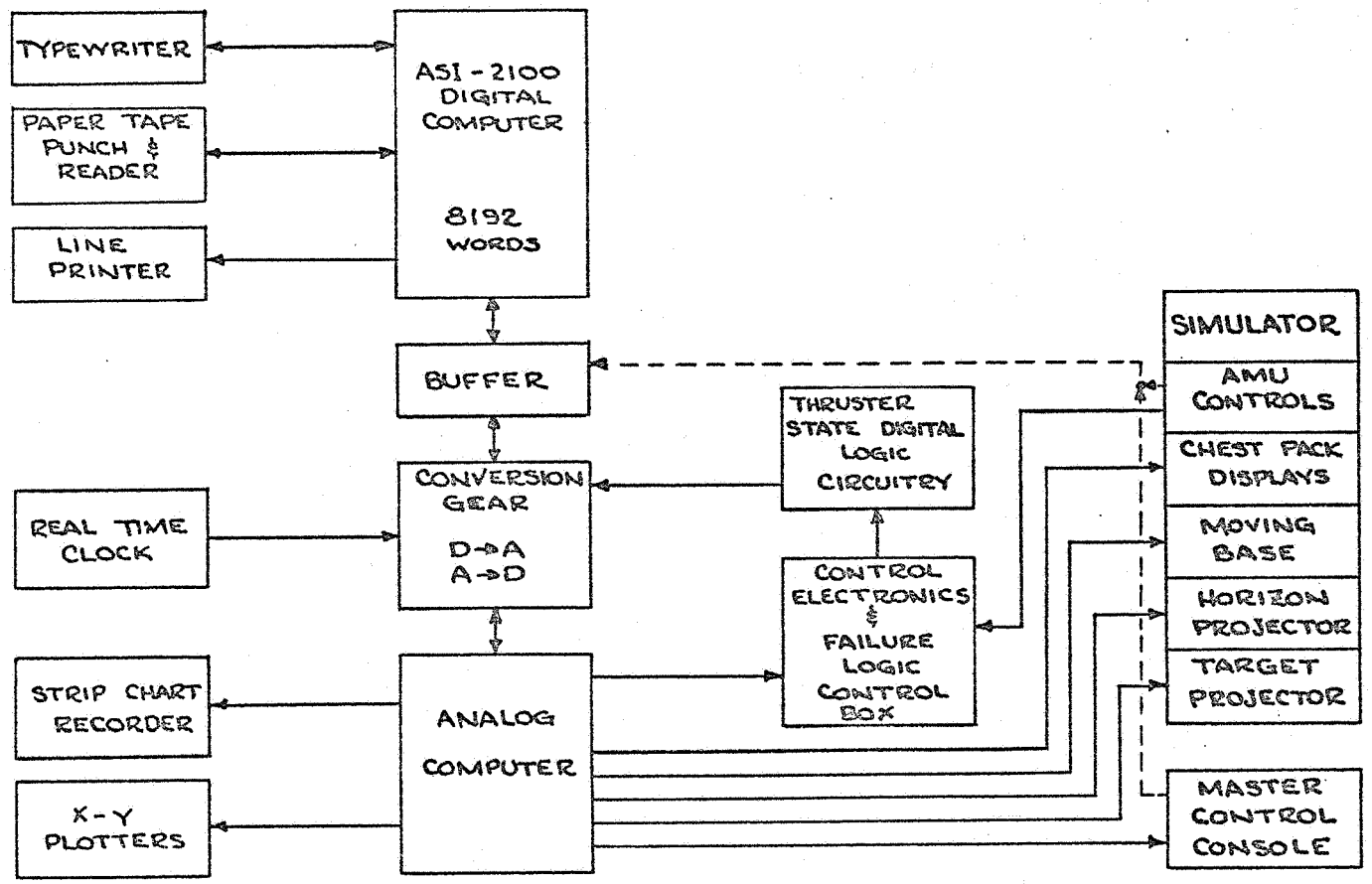

FIGURE 4.1-1 AMU SIMULATOR EQUIPMENT BLOCK DIAGRAM

4.1.4 Suit Pressurization

Installed in the MAFS for pressure suit operation, pressurization and cooling, was a filtered high pressure air supply in combination with a suit pressure regulator and associated hoses and connectors.

4.1.5 Control Electronics and Failure Logic

The primary control electronics package from the AMU backpack installed in the MAFS cockpit was incorporated for the simulation in a special control box, Figure 4.1-2, along with the required electrical power supplies and the thruster and gyro failure mode switching and display logic. The power supplies to the control electronics package and the backpack controllers, rotational and translational, and attitude mode switch were routed through the "on" position of the primary RCS control switch on the backpack. Switches were provided on the control box for failing "on" or "off" each of the eight primary thrusters and each of the three gyro signals. Relays were included which were energized when the alternate RCS control switch on the backpack was in the "on" position. When these relays were energized, all of the failure mode switches were bypassed with thruster and gyro operation then being normal. Thruster failures were produced by interrupting the command signals between the control electronics package and the computer and replacing them with either a steady "on" or steady "off" command. Gyro failures were produced by interrupting the computer simulated rate gyro input signals to the control electronics, they being replaced with either a steady zero (fail "off") or 5 VDC (fail "on") input. In addition to the simulated rate gyro signals, other inputs to the control box, and control electronics, were the rotational and translational controller and attitude mode select, "automatic" or "manual", signals. The control electronics package, as in actuality, supplied the control system logic, thruster pulse modulation, and thruster logic. The outputs of the control box were the basic thruster "on-off" commands as supplied to the computer program.

4.1.6 Master Control Station

Primary control of the simulation program was maintained from the master control station, Figure 4.1-3, located in the computer area. Equipment at this station included the master control console, the control box discussed in paragraph 4.1.5, and the X-Y and strip chart recorders. The master control console housed the primary intercom amplifiers and controls and a number of computer program functional switches. These switches included:

(1) Operate - Reset - Primary control switch for starting and stopping the computer program for each simulation run.

(2) Endpoint - Switch for manually commanding digital data printouts on the line printer, coded "EPT".

(3) N_2 Fail - For initiating fuel (nitrogen supply) pressure failures.

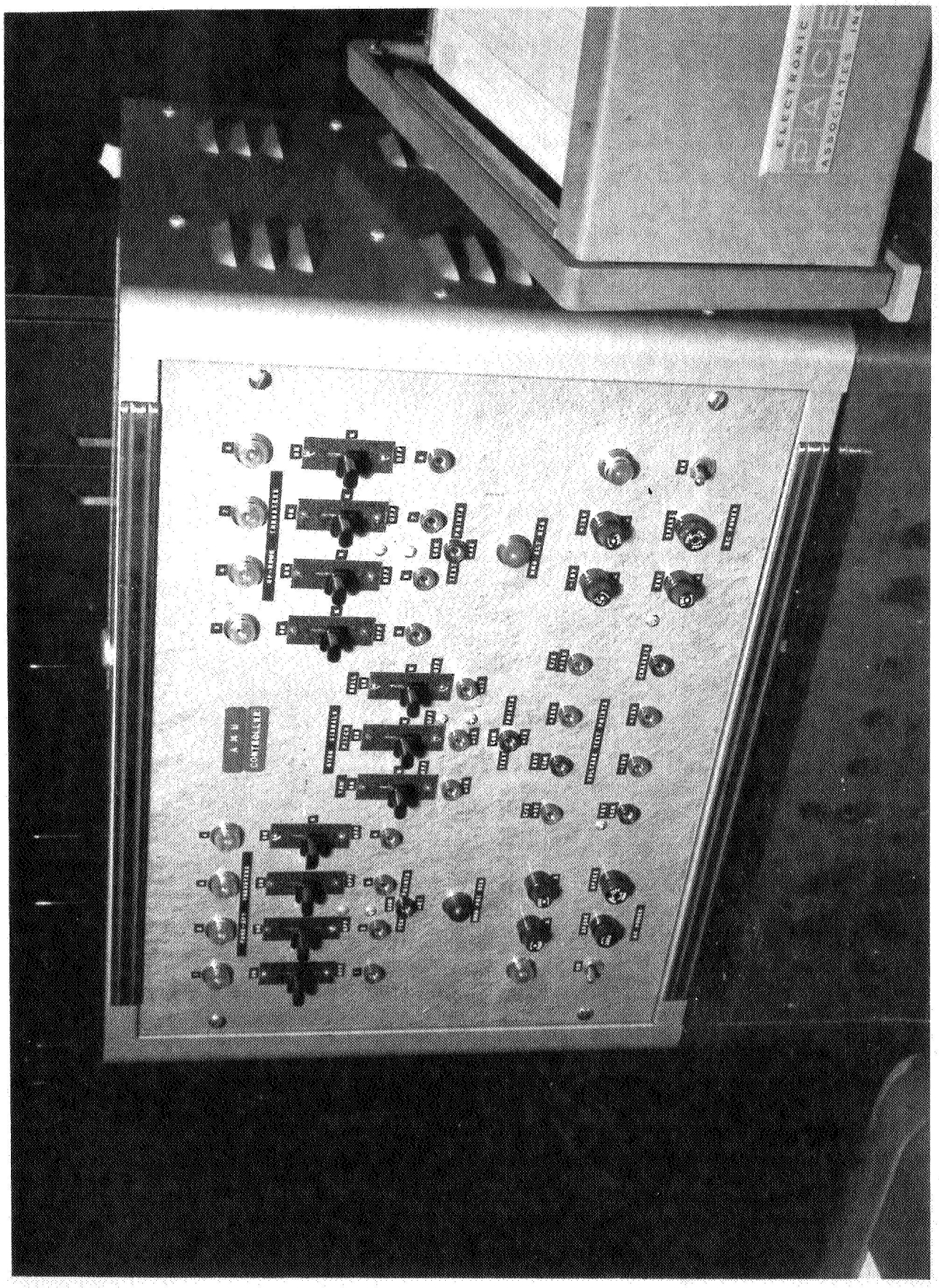

FIG. 4.1-2 AMU CONTROL ELECTRONICS AND FAILURE LOGIC BOX

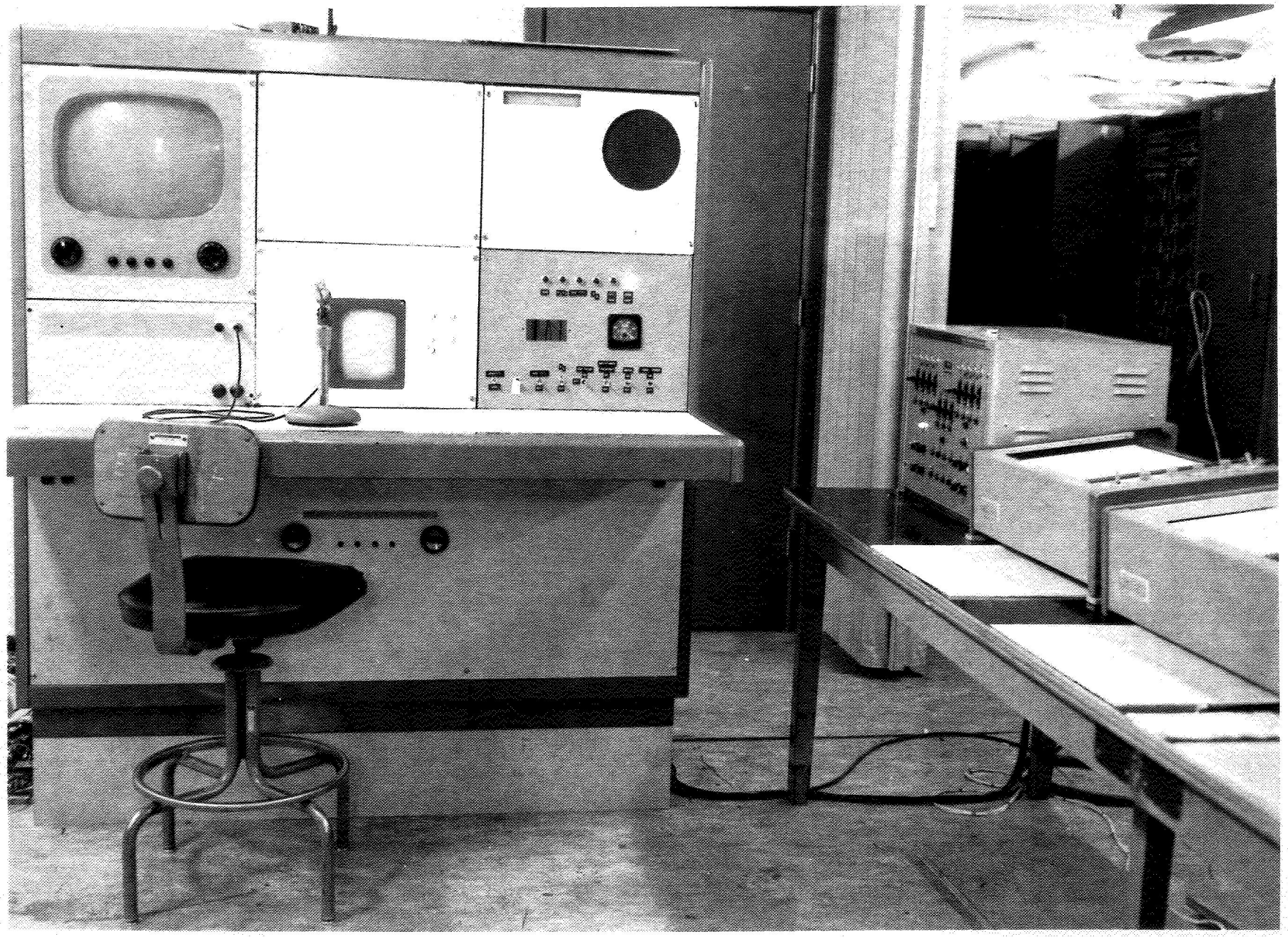

FIG. 4.1-3 AMU SIMULATION - MASTER CONTROL STATION

(4) RCS Fail - Normally used in conjunction with thruster and gyro failures to supply abort alarm, RCS light on chest pack and audio tone on intercom, which was manually operated for this simulation whenever the failures resulted in excessive thruster duty cycles. The abort alarm signal was automatically initiated by the computer when fuel remaining dropped to 30% or for a fuel pressure failure when N_2 pressure dropped to 395 psia.

4.1.7 Computer Equipment

The simulation computations were primarily performed by an ASI-2100 digital computer. This high speed, solid state computer has a 2-microsecond total memory cycle time with 8192 randomly addressable 21 bit words. The complete computer program had a basic iteration rate of 50 milliseconds for the synchronous computations. Asynchronous operation was performed on a priority basis to handle the high frequency pulse modulated thruster commands. Analog computer amplifiers were used to integrate the digitally computed angular acceleration quantities, the outputs simulating the AMU rate gyros. Other analog equipment, using digitally computed parameters, was used to provide the required drive signals for the moving base, visual projection system, fuel remaining display, and X-Y and strip chart recorders. Additional equipment used in conjunction with the computers included:

(1) Conversion Gear - Analog-to-digital and digital-to-analog.

(2) Auxiliary buffer between digital computer and conversion equipment.

(3) Digital typewriter, paper tape reader, and paper tape punch.

(4) Thruster State Digital Interface - Special digital logic circuits to handle each thruster state, pulse decoding, interrupt gating, and time delay for characterizing impulse. Since the computer program utilized square wave thrust pulses, time delays were applied to approximate the impulse characteristics of the minimum width AMU thruster pulse. The delays used were 12 milliseconds for the thruster "on" command and 17 milliseconds for the "off".

(5) Real time clock (oscillator) for timing and gating the digital computer.

4.1.8 Data Recording Equipment

Data recording was performed by a digital line printer, a 12 channel strip chart pen recorder, a 30 x 30 inch dual pen X-Y recorder, and three 11 x 17 inch X-Y recorders.

4.2 EQUATIONS AND TECHNICAL DESCRIPTION

4.2.1 AMU Translation

The absolute translation, position and velocity, of the AMU mass center was determined by solution of differential equations in a geocentric, inertially oriented coordinate system (X_p, Y_p, Z_p) as shown in Figure 4.2-1, the components of inertial acceleration being:

$$\ddot{X}_p = \Delta\ddot{X}_p - \frac{GM}{X_D^3} X_p \tag{1}$$

$$\ddot{Y}_p = \Delta\ddot{Y}_p - \frac{GM}{X_D^3} Y_p \tag{2}$$

$$\ddot{Z}_p = \Delta\ddot{Z}_p - \frac{GM}{X_D^3} Z_p \tag{3}$$

The thrust resultant accelerations ($\Delta\ddot{X}_p$, $\Delta\ddot{Y}_p$, $\Delta\ddot{Z}_p$) were a function of the body axis thrust accelerations and AMU inertial orientation

$$\begin{bmatrix} \Delta\ddot{X}_p \\ \Delta\ddot{Y}_p \\ \Delta\ddot{Z}_p \end{bmatrix} = \begin{bmatrix} l_1 & m_1 & n_1 \\ l_2 & m_2 & n_2 \\ l_3 & m_3 & n_3 \end{bmatrix} \begin{bmatrix} \Delta\ddot{X}_B \\ \Delta\ddot{Y}_B \\ \Delta\ddot{Z}_B \end{bmatrix} \tag{4}$$

with the body axis accelerations being computed from the applied thrusts of the eight primary thrusters located on the AMU as shown in Figure 4.2-2:

$$\Delta\ddot{X}_B = a_x = \frac{1}{m}\left[T_1 + T_2 - T_3 - T_4\right] \tag{5}$$

$$\Delta\ddot{Y}_B = 0 \tag{6}$$

$$\Delta\ddot{Z}_B = a_z = \frac{1}{m}\left[T_5 + T_6 - T_7 - T_8\right] \tag{7}$$

Referring to Figure 4.2-1, AMU geometric definitions included the projection of the AMU local radius vector into the $X_p - Z_p$ plane:

$$X_R = +\sqrt{X_p^2 + Z_p^2} \tag{8}$$

the magnitude of the AMU local radius vector:

$$X_D = +\sqrt{X_R^2 + Y_p^2} \tag{9}$$

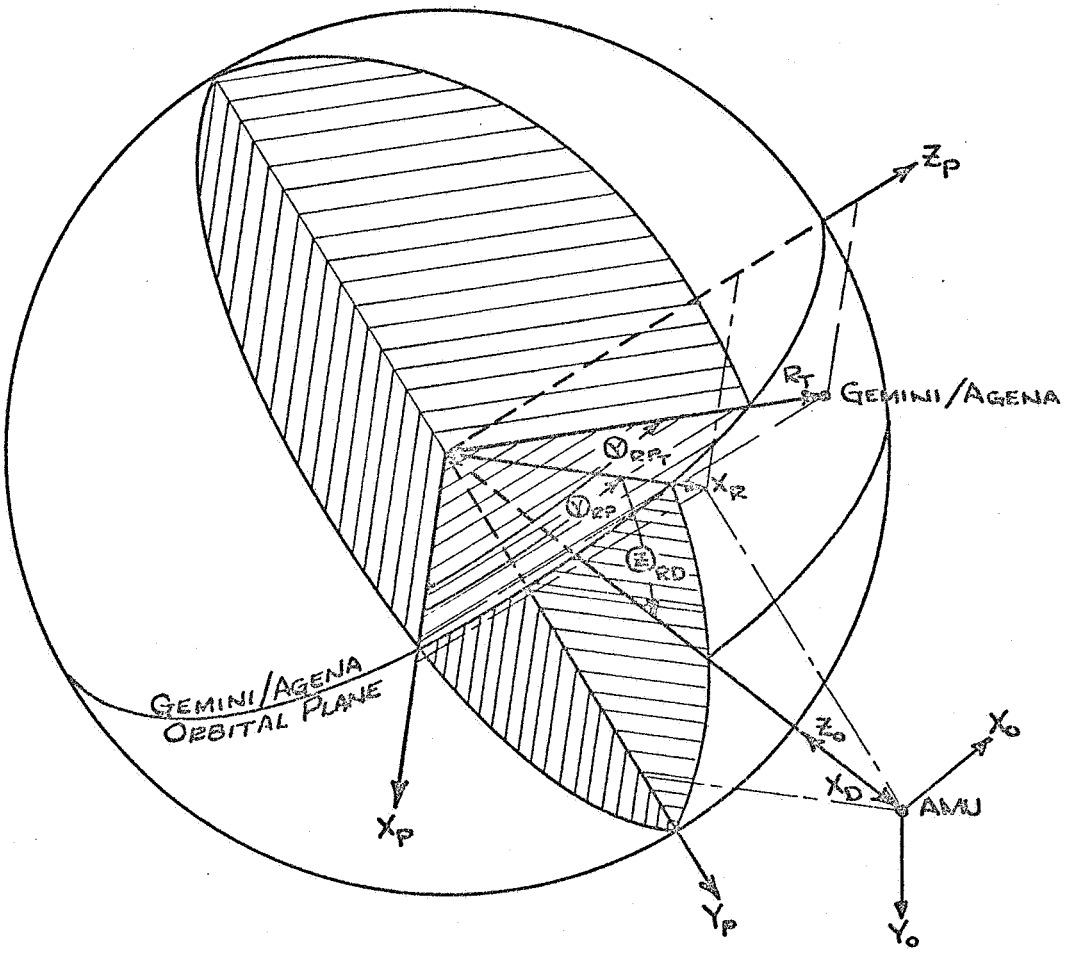

FIGURE 4.2-1 AMU SIMULATION - TRANSLATION GEOMETRY

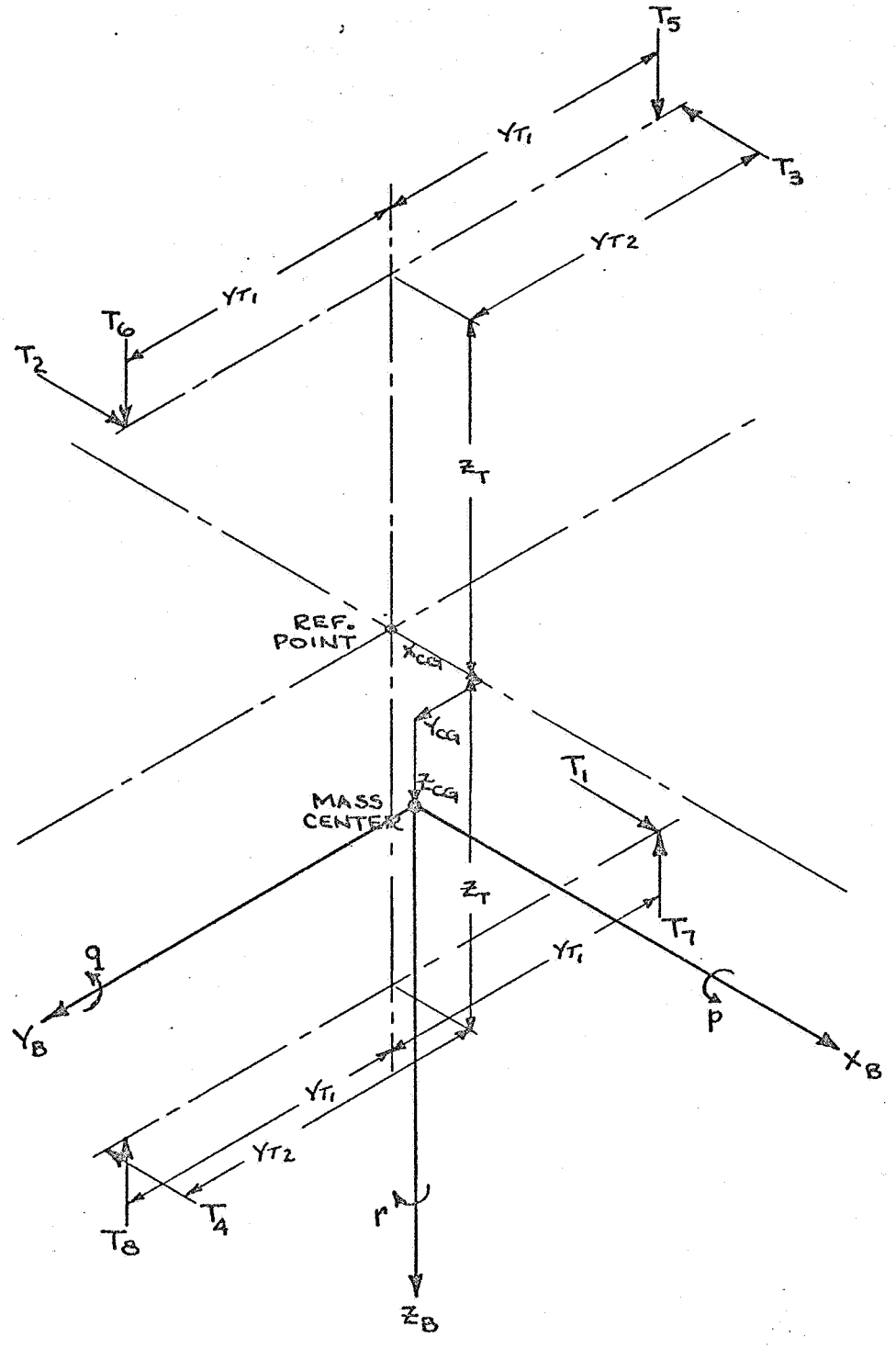

FIGURE 4.2-2 AMU GEOMETRY

the AMU orbital latitude:

$$\sin \textcircled{Z}_{RD} = Y_P / X_D \tag{10}$$

$$\cos \textcircled{Z}_{RD} = X_R / X_D \tag{11}$$

and AMU orbital longitude:

$$\sin \textcircled{Y}_{RP} = Z_P / X_R \tag{12}$$

$$\cos \textcircled{Y}_{RP} = X_P / X_R \tag{13}$$

4.2.2 Gemini/Agena Translation

The Gemini, or Agena, spacecraft was assumed to be in a circular, 160 n. mi. Earth orbit in the inertial X_p - Z_p plane. The absolute translation of the spacecraft, the point mass taken as the center of the nose end, was computed in the inertial coordinate system (X_p, Y_p, Z_p) from:

$$\ddot{X}_{P_T} = - \frac{GM}{R_T^3} X_{P_T} \tag{14}$$

$$\ddot{Y}_{P_T} = \dot{Y}_{P_T} = Y_{P_T} = 0 \tag{15}$$

$$\ddot{Z}_{P_T} = - \frac{GM}{R_T^3} Z_{P_T} \tag{16}$$

Spacecraft longitude was:

$$\sin \textcircled{Y}_{RP_T} = Z_{P_T} / R_T \tag{17}$$

$$\cos \textcircled{Y}_{RP_T} = X_{P_T} / R_T \tag{18}$$

4.2.3 Relative Motion, Inertial Coordinate System

The positions of the Gemini, or Agena, spacecraft point mass relative to the AMU mass center, with respect to the inertial coordinate system, were:

$$R_{X_P} = X_{P_T} - X_P \tag{19}$$

$$R_{Y_P} = -Y_P \tag{20}$$

$$R_{Z_P} = Z_{P_T} - Z_P \tag{21}$$

with the line-of-sight range between the two points being:

$$\rho = +\sqrt{R_{X_P}^2 + R_{Y_P}^2 + R_{Z_P}^2} \tag{22}$$

The inertially oriented relative velocities were:

$$U_{X_P} = \dot{X}_{P_T} - \dot{X}_P \tag{23}$$

$$U_{Y_P} = -\dot{Y}_P \tag{24}$$

$$U_{Z_P} = \dot{Z}_{P_T} - \dot{Z}_P \tag{25}$$

with the resultant being:

$$V_R = +\sqrt{U_{X_P}^2 + U_{Y_P}^2 + U_{Z_P}^2} \tag{26}$$

4.2.4 Relative Motion, Line-of-Sight Coordinate System

The line-of-sight coordinate system, as shown in Figure 4.2-3, was referenced to the AMU body axes (X_B, Y_B, Z_B). The position and velocity components of the spacecraft point mass relative to the AMU mass center in the AMU body axes were determined by:

$$\begin{bmatrix} R_{X_B} \\ R_{Y_B} \\ R_{Z_B} \end{bmatrix} = \begin{bmatrix} l_1 & l_2 & l_3 \\ m_1 & m_2 & m_3 \\ n_1 & n_2 & n_3 \end{bmatrix} \begin{bmatrix} R_{X_P} \\ R_{Y_P} \\ R_{Z_P} \end{bmatrix} \tag{27}$$

$$\begin{bmatrix} U_{X_B} \\ U_{Y_B} \\ U_{Z_B} \end{bmatrix} = \begin{bmatrix} l_1 & l_2 & l_3 \\ m_1 & m_2 & m_3 \\ n_1 & n_2 & n_3 \end{bmatrix} \begin{bmatrix} U_{X_P} \\ U_{Y_P} \\ U_{Z_P} \end{bmatrix} \tag{28}$$

These quantities were then used to compute the line-of-sight polar angles, range (ρ) already defined by equation (22):

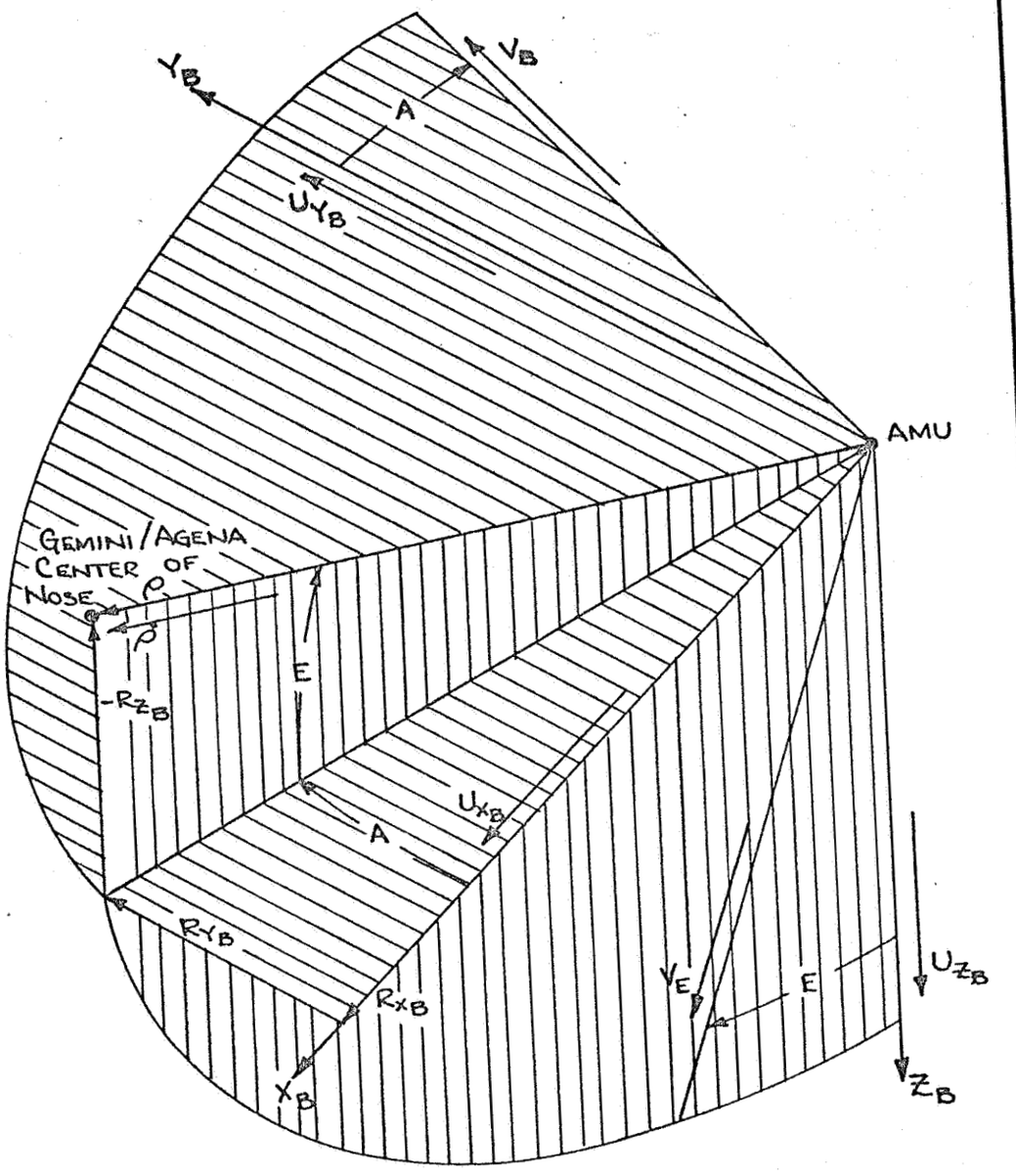

FIGURE 4.2-3 LINE-OF-SIGHT COORDINATE SYSTEM

$$\sin E = -R_{Z_B}/\rho \tag{29}$$

$$\cos E = +\sqrt{R_{X_B}^2 + R_{Y_B}^2}\,/\rho \tag{30}$$

$$\sin A = R_{Y_B}/\rho \cos E \tag{31}$$

$$\cos A = R_{X_B}/\rho \cos E \tag{32}$$

and the line-of-sight velocity components:

$$\begin{bmatrix} \dot{\rho} \\ V_B \\ V_E \end{bmatrix} = \begin{bmatrix} \cos E & 0 & -\sin E \\ 0 & 1 & 0 \\ \sin E & 0 & \cos E \end{bmatrix} \begin{bmatrix} \cos A & \sin A & 0 \\ -\sin A & \cos A & 0 \\ 0 & 0 & 1 \end{bmatrix} \begin{bmatrix} U_{X_B} \\ U_{Y_B} \\ U_{Z_B} \end{bmatrix} \tag{33}$$

4.2.5 AMU Rotation

The angular accelerations of the AMU were computed in the body axes from simultaneous solutions of:

$$I_x \dot{p} - I_{xy}\dot{q} - I_{xz}\dot{r} = L - (I_z - I_y)qr + I_{yz}(q^2 - r^2) + I_{xz}pq - I_{xy}pr \tag{34}$$

$$-I_{xy}\dot{p} + I_y\dot{q} - I_{yz}\dot{r} = M - (I_x - I_z)pr + I_{xz}(r^2 - p^2) + I_{xy}qr - I_{yz}pq \tag{35}$$

$$-I_{xz}\dot{p} - I_{yz}\dot{q} + I_z\dot{r} = N - (I_y - I_x)pq + I_{xy}(p^2 - q^2) + I_{yz}pr - I_{xz}qr \tag{36}$$

where the body axis moments, from the geometry of Figure 4.2-2, were defined by:

$$L = (T_6 + T_7 - T_5 - T_8)Y_{T_1} - ma_z Y_{CG} \tag{37}$$

$$M = (T_1 + T_3 - T_2 - T_4)Z_T - ma_x Z_{CG} + ma_z X_{CG} \tag{38}$$

$$N = (T_1 - T_2)Y_{T_1} + (T_4 - T_3)Y_{T_2} + ma_x Y_{CG} \tag{39}$$

4.2.6 AMU Orientation

The direction cosines, defining AMU orientation relative to the inertial axes, were determined from:

$$\begin{bmatrix} \dot{l}_1 & \dot{m}_1 & \dot{n}_1 \\ \dot{l}_2 & \dot{m}_2 & \dot{n}_2 \\ \dot{l}_3 & \dot{m}_3 & \dot{n}_3 \end{bmatrix} = \begin{bmatrix} l_1 & m_1 & n_1 \\ l_2 & m_2 & n_2 \\ l_3 & m_3 & n_3 \end{bmatrix} \begin{bmatrix} 0 & -r & q \\ r & 0 & -p \\ -q & p & 0 \end{bmatrix} \tag{40}$$

To compute the Euler angles for the horizon projector drive signals required the direction cosines relating the AMU body axes to the AMU local vertical axes (X_0, Y_0, Z_0), shown in Figure 4.2-1:

$$\begin{bmatrix} -l_{o_3} & -m_{o_3} & -n_{o_3} \\ l_{o_2} & m_{o_2} & n_{o_2} \\ l_{o_1} & m_{o_1} & n_{o_1} \end{bmatrix} = \begin{bmatrix} \cos\Theta_{RD} & \sin\Theta_{RD} & 0 \\ -\sin\Theta_{RD} & \cos\Theta_{RD} & 0 \\ 0 & 0 & 1 \end{bmatrix} \begin{bmatrix} \cos\Theta_{RP} & 0 & \sin\Theta_{RP} \\ 0 & 1 & 0 \\ -\sin\Theta_{RP} & 0 & \cos\Theta_{RP} \end{bmatrix} \begin{bmatrix} l_1 & m_1 & n_1 \\ l_2 & m_2 & n_2 \\ l_3 & m_3 & n_3 \end{bmatrix} \tag{41}$$

The four drive angles for the horizon projector were then computed from the direction cosines of equation (40) and the yaw angle of the corresponding three-angle Euler set, both sets being illustrated in Figure 4.2-4:

$$\sin\Psi_3 = l_{o_2} / +\sqrt{1 - l_{o_3}^2} \tag{42}$$

$$\cos\Psi_3 = l_{o_1} / +\sqrt{1 - l_{o_3}^2} \tag{43}$$

$$\dot{\Psi}_4 = \left[K_\Psi (\Psi_3 - \Psi_4) \right]_{\text{lim} \pm \dot{\Psi}_{4\,MAX}} \tag{44}$$ *

$$\tan\phi_{R_4} = \frac{l_{o_1}\sin\Psi_4 - l_{o_2}\cos\Psi_4}{l_{o_3}} \tag{45}$$

$$\sin\Theta_4 = -l_{o_3} / \cos\phi_{R_4} \tag{46}$$

$$\cos\Theta_4 = l_{o_1}\cos\Psi_4 + l_{o_2}\sin\Psi_4 \tag{47}$$

* Equation 44 revised 9-20-66

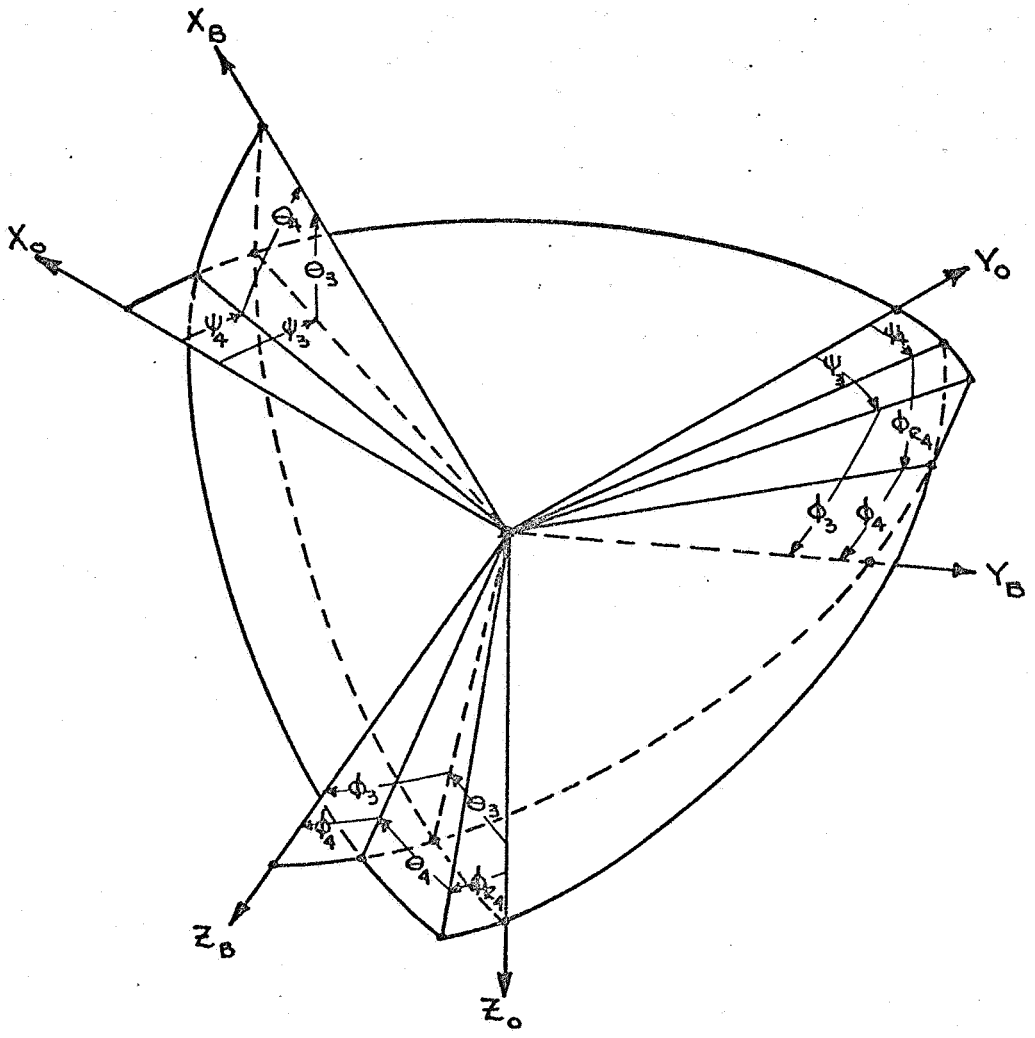

3-Angle Euler Convention $\Psi_3 \rightarrow \Theta_3 \rightarrow \phi_3$

4-Angle Euler Convention (Horizon Projector)

$\Psi_4 \rightarrow \phi_{R4} \rightarrow \Theta_4 \rightarrow \phi_4$

Figure 4.2-4 Euler Angle Geometry

$$\sin\phi_4 = n_{o_1}\cos\phi_{R_4}\sin\psi_4 - n_{o_2}\cos\phi_{R_4}\cos\psi_4 - n_{o_3}\sin\phi_{R_4} \quad (48)$$

$$\cos\phi_4 = -m_{o_1}\cos\phi_{R_4}\sin\psi_4 + m_{o_2}\cos\phi_{R_4}\cos\psi_4 + m_{o_3}\sin\phi_{R_4} \quad (49)$$

The gain, K_ψ , and limit, $\dot{\psi}_{4\ max}$, were adjusted to match the slew capabilities of the projector yaw, ψ_4 , and primary roll, ϕ_4 , drives with redundant roll, ϕ_{R_4} , displacements no greater than the physical limit of ±20 degrees.

4.2.7 Thrust Level

The thrust level was set independently for each thruster, the normal levels corresponding to measured values from tests of AMU No. 17. The thrust levels were constant except for fuel pressure failure cases when thrust would deteriorate with decreasing pressure. The thrust levels were computed from the normal levels and the thrust correction factor:

$$T_j = K_T T_{j_N} \quad (50)$$

where the subscript "j" refers to thruster number, 1,2,3 --- 8, and the thrust correction factor, a function of fuel pressure, was computed by:

$$K_T = 1 - 0.001605(455 - P_N) \quad (51)$$

4.2.8 Fuel and Mass Computation

The fuel consumed by each thruster for each pulse was separately computed:

$$\Delta m_j = \frac{T_j}{32.2\ I_{SP}}\ t_{ON} \quad (52)$$

where t_{ON} was the actual thruster on time determined from the commanded on time and the applied time delays - the t_{ON} value being 5 milliseconds longer than the commanded on time.

Total fuel consumed by the eight thrusters at any instant in the run was:

$$\Delta m_{RCS} = \sum_1^\infty \Delta m_j \quad (53)$$

Translational fuel used along each axis, X_B and Z_B was:

$$\Delta m_x = \int_0^t \frac{m|a_x|}{32.2\, I_{sp}}\, dt \tag{54}$$

$$\Delta m_z = \int_0^t \frac{m|a_z|}{32.2\, I_{sp}}\, dt \tag{55}$$

with total fuel for translation being:

$$\Delta m_{TR} = \Delta m_x + \Delta m_z \tag{56}$$

and for rotation:

$$\Delta m_{ROT} = \Delta m_{RCS} - \Delta m_{TR} \tag{57}$$

The instantaneous AMU mass was:

$$m = m_o - \Delta m_{RCS} \tag{58}$$

The translational ΔV requirement was computed from:

$$\Delta V_{TR} = \int_0^t (|a_x| + |a_z|)\, dt \tag{59}$$

4.2.9 Target Projector Equations

The visual display projection system, by means of the two circular spots (blue and red), represented the two ends of the Gemini or Agena spacecraft. The computer program was such that either target vehicle could be aligned with the longitudinal axis either in the orbital plane or normal to it, illustrated in Figure 4.2-5. For the normal condition the nose end of each spacecraft was considered to be in the orbital plane, the Gemini aligned to face orbital north and the Agena orbital south. The spacecraft could be rotated about that axis which was normal to the orbital plane, lateral or longitudinal, which in each case was designated as the Y_T axis.

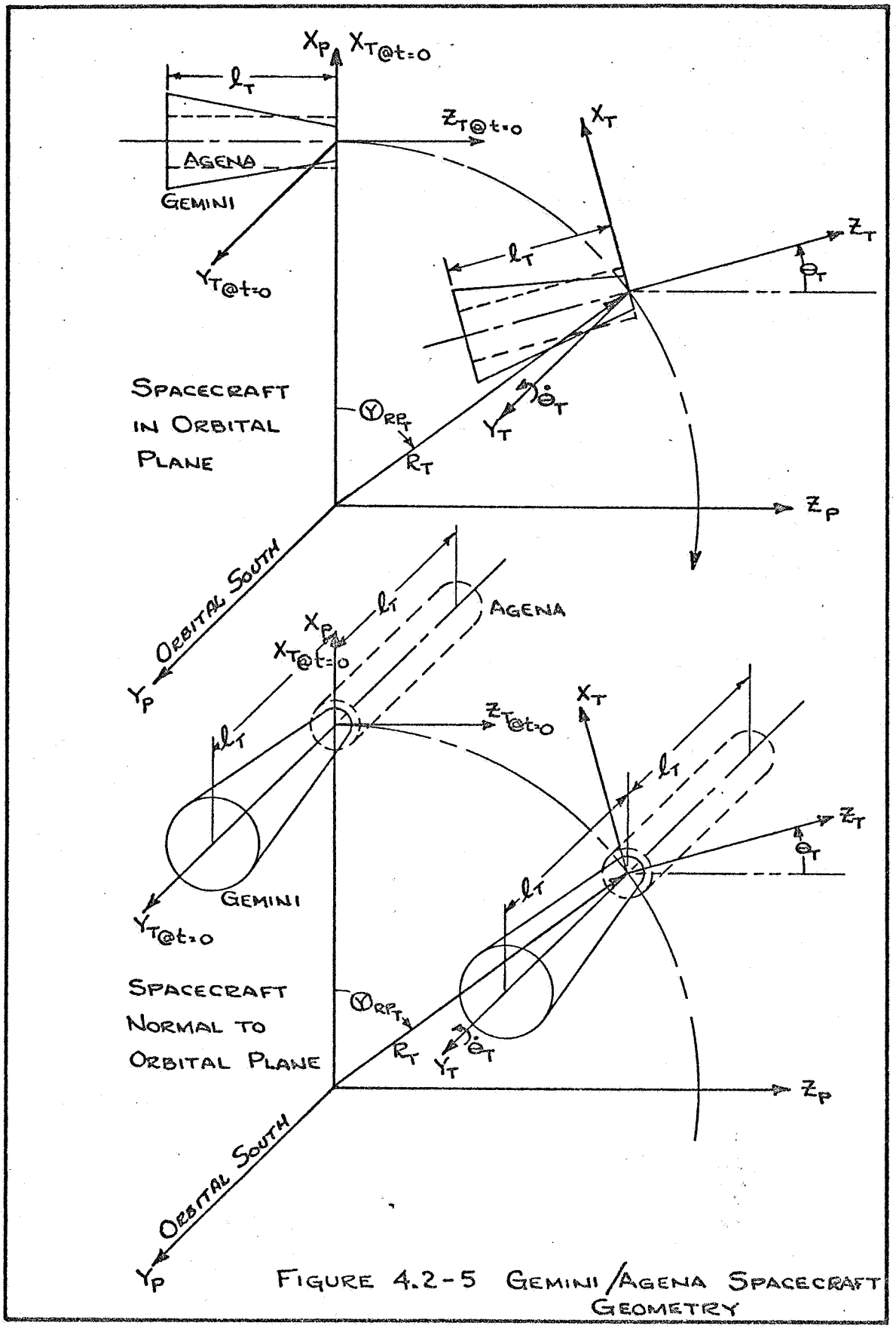

FIGURE 4.2-5 GEMINI/AGENA SPACECRAFT GEOMETRY

The rotation rate could be either zero or some other constant, $\dot{\Theta}_T$, which was preset prior to a run. The inertial displacement about the Y_T (or Y_p) axis was a function of run time, the X_T, Y_T, Z_T axes always coinciding with the X_p, Y_p, Z_p axes at the start of a run.

$$\Theta_T = \dot{\Theta}_T \, t \tag{60}$$

Figure 4.2-6 defines the target projector geometry. The outer azimuth and elevation gimbals of the target projector positioned the spot (blue) which represented the nose end of each spacecraft and were driven by the line-of-sight azimuth and elevation angles from equations (29) - (32). Incremental azimuth and elevation angles for driving the inner projector gimbals which positioned the spot (red) representing the aft end were computed from:

$$\tan \Delta A = \frac{\Delta R_B}{\rho + \Delta\rho} \tag{61}$$

$$\tan \Delta E = \frac{-\Delta R_E \cos \Delta A}{\rho + \Delta\rho} \tag{62}$$

where:

$$\begin{bmatrix} \Delta\rho \\ \Delta R_B \\ \Delta R_E \end{bmatrix} = \begin{bmatrix} \cos E & 0 & -\sin E \\ 0 & 1 & 0 \\ \sin E & 0 & \cos E \end{bmatrix} \begin{bmatrix} \cos A & \sin A & 0 \\ -\sin A & \cos A & 0 \\ 0 & 0 & 1 \end{bmatrix} \begin{bmatrix} \Delta R_{X_B} \\ \Delta R_{Y_B} \\ \Delta R_{Z_B} \end{bmatrix} \tag{63}$$

The values of ΔR_{X_B}, ΔR_{Y_B}, and ΔR_{Z_B} were functions of target length, ℓ_T, and orientation. The length, ℓ_T, was the same for both the Gemini and Agena spacecraft, 18.67 ft.

$$\begin{bmatrix} \Delta R_{X_B} \\ \Delta R_{Y_B} \\ \Delta R_{Z_B} \end{bmatrix} = \begin{bmatrix} \ell_1 & \ell_2 & \ell_3 \\ m_1 & m_2 & m_3 \\ n_1 & n_2 & n_3 \end{bmatrix} \begin{bmatrix} \cos\Theta_T & 0 & \sin\Theta_T \\ 0 & 1 & 0 \\ -\sin\Theta_T & 0 & \cos\Theta_T \end{bmatrix} \begin{bmatrix} M_L \end{bmatrix} \tag{64}$$

where $[M_L]$ was:

(1) Gemini or Agena in orbital plane

$$[M_L] \triangleq \begin{bmatrix} 0 \\ 0 \\ -\ell_T \end{bmatrix} \tag{65-1}$$

(2) Gemini normal to orbital plane

$$[M_L] \triangleq \begin{bmatrix} 0 \\ \ell_T \\ 0 \end{bmatrix} \tag{65-2}$$

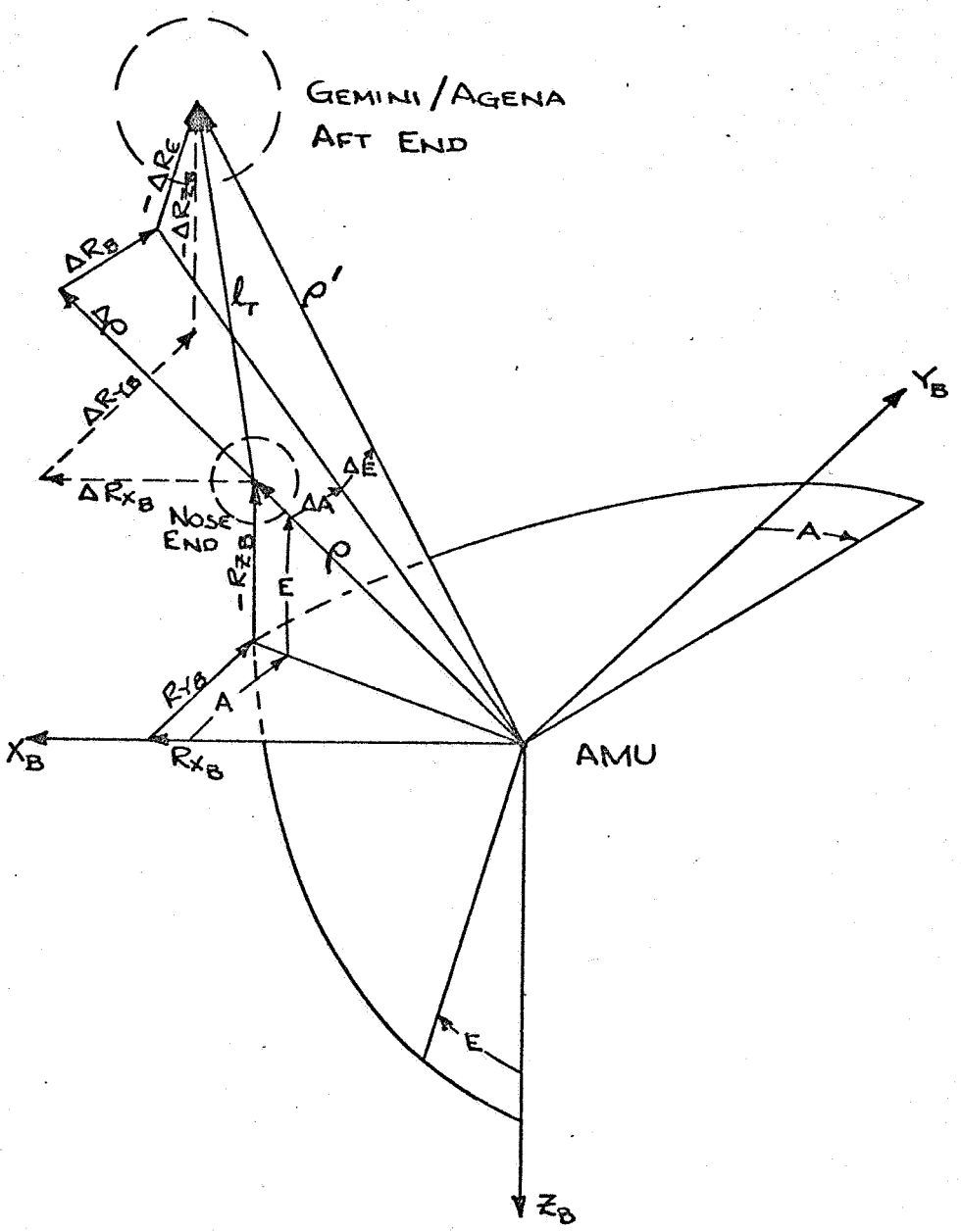

FIGURE 4.2-6 TARGET PROJECTOR GEOMETRY

(3) Agena normal to orbital plane

$$[M_L] \triangleq \begin{bmatrix} 0 \\ -\ell_T \\ 0 \end{bmatrix} \tag{65-3}$$

The line-of-sight range to the nose end of the spacecraft (ρ) has been defined by equation (22). The range to the aft end was computed by:

$$\rho' = \frac{\rho + \Delta\rho}{\cos\Delta A \cos\Delta E} \tag{66}$$

The diameter of the nose end spot (D_{SPOT}) and aft end spot (d_{SPOT}) for use in the target projector drives were:

$$D_{SPOT} = \frac{8\, D_{REF}}{\rho\,(feet)} \tag{67}$$

$$d_{SPOT} = \frac{8\, d_{REF}}{\rho'\,(feet)} \tag{68}$$

where D_{REF} and d_{REF} were 40 and 120 inches, respectively, for the Gemini spacecraft, and both D_{REF} and d_{REF} were 60 inches for the Agena. Compensations for physical geometry since the target projector to screen distance varies with projector orientation were made to all of the computed parameters (A,E, ΔA, ΔE, D_{SPOT} and d_{SPOT}) prior to driving the projector.

4.2.10 Relative Motion, Spacecraft Coordinates

Recorded data parameters of relative position (X-Y plotters plus line printer) and velocity (line printer) components were presented in the Gemini/Agena spacecraft referenced coordinate system (X_T, Y_T, Z_T). These parameters, which like all other relative motion terms in this simulation denoted spacecraft motion relative to the AMU, were computed from:

$$\begin{bmatrix} R_{X_T} \\ R_{Y_T} \\ R_{Z_T} \end{bmatrix} = \begin{bmatrix} \cos\theta_T & 0 & -\sin\theta_T \\ 0 & 1 & 0 \\ \sin\theta_T & 0 & \cos\theta_T \end{bmatrix} \begin{bmatrix} R_{X_P} \\ R_{Y_P} \\ R_{Z_P} \end{bmatrix} \tag{69}$$

$$\begin{bmatrix} U_{X_T} \\ U_{Y_T} \\ U_{Z_T} \end{bmatrix} = \begin{bmatrix} \cos\theta_T & 0 & -\sin\theta_T \\ 0 & 1 & 0 \\ \sin\theta_T & 0 & \cos\theta_T \end{bmatrix} \begin{bmatrix} U_{X_P} \\ U_{Y_P} \\ U_{Z_P} \end{bmatrix} \tag{70}$$

For the majority of the runs in this program, for all of the astronaut training runs, $\dot{\Theta}_T$ was set equal to a negative value of the rate of change of Θ_{RP_T} to maintain the X_T and Z_T axes in the spacecraft local vertical and horizontal, respectively. Since the astronaut runs were all made with the spacecraft longitudinal axes normal to the orbital plane, this rotation was about the axis of symmetry and had no effect on the visual display.

4.2.11 Moving Base Drives

The moving base drive signals were computed from:

$$\text{Roll Drive} = \left[\frac{0.3\dot{p}}{2s+1}\right]_{\text{lim} \pm .349 \text{ rad}} \tag{71}$$

$$\text{Inner Pitch Drive} = \left[\frac{\frac{-.05q_I(.1s)}{.1s+1} + .05\dot{q}\,X_{PILOT}}{2s+1}\right]_{\text{lim} \pm .174 \text{ rad}} \tag{72}$$

$$\text{Yaw Drive} = \left[\frac{.05\left(\dot{r}\,X_{PILOT} - \dot{p}\,Z_{PILOT}\right)}{2s+1}\right]_{\text{lim} \pm .174 \text{ rad}} \tag{73}$$

4.2.12 Fuel Pressure Computation

The fuel (nitrogen supply) pressure was constant unless a failure was simulated. The pressure then was computed for an isothermal expansion by:

$$P_N = \frac{455\,V_o}{V} \tag{74}$$

Where the initial ullage volume at the time of failure occurrence was V_o with the instantaneous volume computed by:

$$V = 44.8 + \frac{\Delta m_{RCS}}{0.0493} \tag{75}$$

4.2.13 Definition of Symbols

Symbol	Definition
A	Line-of-sight (LOS) azimuth angle - AMU body axis oriented.
ΔA	Differential LOS azimuth between Gemini/Agena spacecraft nose and aft ends.
a_x, a_z	Thrust resultant translational accelerations - AMU X_B and Z_B body axes.
D_{REF}, d_{REF}	Reference diameters of spacecraft nose and aft ends, respectively.
D_{SPOT}, d_{SPOT}	Target projector drive signals for diameters of spots representing spacecraft nose and aft ends, respectively.
E	LOS elevation angle - AMU body axis oriented.
ΔE	Differential LOS elevation between spacecraft nose and aft ends.
GM	Earth gravitational constant.
I_{SP}	Specific impulse.
I_x, I_y, I_z	Principal moments of inertia, AMU body axes.
I_{xy}, I_{xz}, I_{yz}	Products of inertia, AMU body axes.
K_T	Thrust correction factor for reduced fuel pressure.
K_ψ	Gain term in 4-angle Euler set yaw computation.
L, M, N	Rotational moments about AMU body axes.
$l_{1,2,3}\ m_{1,2,3}\ n_{1,2,3}$	Direction cosines - AMU body to inertial axes.
$\dot{l}_{1,2,3}\ \dot{m}_{1,2,3}\ \dot{n}_{1,2,3}$	Inertial direction cosine rates.
$l_{o_{1,2,3}}\ m_{o_{1,2,3}}\ n_{o_{1,2,3}}$	Direction cosines - AMU body to AMU local vertical axes.

Symbol	Definition
ℓ_T	Gemini/Agena spacecraft length - reference distance between centers of nose and aft ends.
m	Instantaneous AMU mass.
m_o	Initial AMU mass.
$[M_L]$	Spacecraft length matrix in target projector computations.
Δm_j	Incremental fuel consumption for each thruster pulse, subscript "j" representing thruster number (1, 2, 3 ---8).
Δm_{RCS}	Instantaneous total fuel consumption.
Δm_{ROT}	Instantaneous rotational fuel consumption.
Δm_{TR}	Instantaneous translational fuel consumption.
$\Delta m_x, \Delta m_z$	Instantaneous translation fuel consumption components, AMU X_B and Z_B body axes.
p, q, r	Angular rates about AMU body axes.
$\dot{p}, \dot{q}, \dot{r}$	Angular accelerations about AMU body axes.
P_N	Fuel, nitrogen supply, pressure.
R_T	Gemini/Agena radius from center of Earth.
$R_{X_B}, R_{Y_B}, R_{Z_B}$	Components of spacecraft position relative to AMU - AMU body axes.
$R_{X_P}, R_{Y_P}, R_{Z_P}$	Components of spacecraft position relative to AMU - inertial axes.
$R_{X_T}, R_{Y_T}, R_{Z_T}$	Components of spacecraft position relative to AMU - spacecraft referenced axes.

Symbol	Definition
$\Delta R_B, \Delta R_E, \Delta\rho$	Differential position components between spacecraft nose and aft ends - LOS coordinate system.
$\Delta R_{X_B}, \Delta R_{Y_B}, \Delta R_{Z_B}$	Differential position components between spacecraft nose and aft ends - AMU body axes.
s	Laplace operator.
$T_{1,2,3\cdots 8}$	Instantaneous thrust levels of each primary thruster.
T_j	Instantaneous thrust level, subscript "j" representing thruster number (1, 2, 3 --- 8).
T_{j_N}	Normal thrust level of each thruster.
t	Elapsed time in run.
t_{on}	Applied length of thruster pulse.
$U_{X_B}, U_{Y_B}, U_{Z_B}$	Components of spacecraft velocity relative to AMU - AMU body axes.
$U_{X_P}, U_{Y_P}, U_{Z_P}$	Components of spacecraft velocity relative to AMU - inertial axes.
$U_{X_T}, U_{Y_T}, U_{Z_T}$	Components of spacecraft velocity relative to AMU - spacecraft referenced axes.
V	Instantaneous ullage volume.
V_o	Ullage volume at time of fuel pressure failure occurrence.
V_B, V_E	Components of spacecraft velocity relative to AMU - normal to line-of-sight.
V_R	Resultant relative velocity.
ΔV_{TR}	Translation ΔV requirement.
X_{CG}, Y_{CG}, Z_{CG}	AMU mass center displacements from reference point.

Symbol	Definition
X_D	AMU radius from center of Earth.
X_P, Y_P, Z_P	Components of AMU inertial position.
$X_{P_T}, Y_{P_T}, Z_{P_T}$	Components of spacecraft inertial position.
$\dot{X}_P, \dot{Y}_P, \dot{Z}_P$	Components of AMU inertial velocity.
$\dot{X}_{P_T}, \dot{Y}_{P_T}, \dot{Z}_{P_T}$	Components of spacecraft inertial velocity.
$\ddot{X}_P, \ddot{Y}_P, \ddot{Z}_P$	Components of AMU inertial acceleration.
$\ddot{X}_{P_T}, \ddot{Y}_{P_T}, \ddot{Z}_{P_T}$	Components of spacecraft inertial acceleration.
X_{PILOT}, Z_{PILOT}	Pilot mass center displacements from AMU mass center.
X_R	Projection of AMU radius from center of Earth into X_P - Z_P plane.
$\Delta\ddot{X}_B, \Delta\ddot{Y}_B, \Delta\ddot{Z}_B$	Thrust resultant translational accelerations - AMU body axes.
$\Delta\ddot{X}_P, \Delta\ddot{Y}_P, \Delta\ddot{Z}_P$	Thrust resultant translational accelerations - inertial axes.
Y_{T_1}, Y_{T_2}	Lateral displacement of inboard and outboard thrusters, respectively, from reference point.
Z_T	Vertical displacement of fore-aft thrusters from reference point.
$\textcircled{Y}_{RP}$	AMU orbital longitude.
$\textcircled{Y}_{RP_T}$	Gemini/Agena orbital longitude.
$\textcircled{Z}_{RD}$	AMU orbital latitude.
$\Theta_T, \dot{\Theta}_T$	Inertial angular displacement and rate of spacecraft about Y_T axis.

Symbol	Definition
ρ	LOS range - AMU from center of spacecraft nose end.
ρ'	LOS range - AMU from center of spacecraft aft end.
$\dot{\rho}$	LOS range rate - $d\rho/dt$
ψ_3	3-angle Euler set yaw angle - AMU orientation in local horizontal.
$\psi_4, \phi_{R4}, \theta_4, \phi_4$	4-angle Euler set - AMU orientation in local vertical-horizontal.
$\dot{\psi}_4$	4-angle Euler set yaw angle rate.
$\dot{\psi}_{4\,MAX}$	Computational limit on $\dot{\psi}_4$.

4.3 DATA RECORDING

4.3.1 Analog Recording

A 12-channel strip chart pen recorder was utilized to record the following parameters as functions of time:

$\dot{p}$	a_x
$\dot{q}$	a_z
$\dot{r}$	$\dot{\rho}$
p	Fore-Aft Transl. Cmd.
q	RCS Failure Indication
r	Attitude Control Mode

Three 11 x 17 inch and one 30 x 30 inch, dual pen, X-Y recorders were used for recording and/or displaying the following:

(1) R_{XT} vs. R_{ZT}

(2) R_{YT} vs. R_{ZT}

(3) R_{XT} vs. R_{YT}

(4) $\dot{\rho}$ vs. ρ

(5) V_E vs. V_B

Permanent records were made for selected runs with only the first three recorders. Automatic scale changes occurred on the parameters for the first three plus ρ on the fourth, all four parameters changing scale simultaneously as a function of LOS range, ρ . Three scales were used - 0 to 32 ft., 0 to 256 ft., and 0 to 2048 ft..

4.3.2 Digital Recording

A line printer was utilized for on-line recording of 32 digital parameters accomplished on an event or manual command basis with the appropriate index code appearing with each data printout. The index code used was:

Index	Definition
OPR	Operate - Start of Run
ATO	Automatic Control Mode Initiate
OLP	Manual (Open Loop) Control Mode Initiate
FTR	Translation Command Initiate
STR	Translation Command Terminate

Index	Definition
PRC	Roll Command Initiate
PRS	Roll Command Terminate
QRC	Pitch Command Initiate
QRS	Pitch Command Terminate
RRC	Yaw Command Initiate
RRS	Yaw Command Terminate
N2F	Fuel Pressure Failure Initiate
EPT	End Point - Manual Commanded Printout

The event printouts for rotation commands could be disabled by a switch on the command console. The 32 parameters on each printout were:

t sec	Φ_{RP_T} deg	R_{XT} ft	R_{YT} ft	R_{ZT} ft	U_{XT} fps	U_{YT} fps	U_{ZT} fps
ρ ft	$\dot{\rho}$ fps	V_E fps	V_B fps	A deg	E deg	V_R fps	θ_T deg
m lbm	Δm_{RCS} lbm	Δm_{ROT} lbm	Δm_{TR} lbm	Δm_X lbm	Δm_Z lbm	ΔV_{TR} fps	P_N psia
TOTAL PULSES FOR EACH THRUSTER							
1	2	3	4	5	6	7	8

4.4 AMU CONFIGURATION AND INITIAL CONDITION DATA

The AMU configuration parameters which were constant for every run were:

Parameter	Value
Normal Thrust Levels	
Thruster 1	2.125 lb
Thruster 2	2.338 lb
Thruster 3	2.275 lb
Thruster 4	2.190 lb
Thruster 5	2.076 lb
Thruster 6	2.280 lb
Thruster 7	2.325 lb
Thruster 8	2.249 lb
I_{SP}	150 sec
Y_{T_1}	0.8 ft

Parameter	Value	
Y_{T_2}	0.904167	ft
Z_T	1.1125	ft
Initial Fuel Quantity	23.65	lbm

Other AMU configuration data which were different for each astronaut were:

Parameter	Value		
	Cernan	Aldrin	
m_0	12.655 (407.5)	12.500 (402.5)	slugs (lbm)
X_{CG}	0.175	0.158	ft
Y_{CG}	-0.008	-0.008	ft
Z_{CG}	0.216	0.150	ft
I_X	20.22	19.06	slug-ft^2
I_Y	22.92	21.62	slug-ft^2
I_Z	8.97	8.49	slug-ft^2
I_{XY}	-0.09	-0.09	slug-ft^2
I_{XZ}	1.72	1.25	slug-ft^2
I_{YZ}	-0.07	-0.02	slug-ft^2
X_{PILOT}	0.317	0.317	ft
Z_{PILOT}	0.358	0.350	ft

Miscellaneous constants on all runs were:

Parameter	Value	
GM	1.4077345×10^{16}	ft^3/sec^2
ℓ_T	18.67	ft
R_T	21.898824×10^6	ft
$\dot{\theta}_T$	$-1.157788381 \times 10^{-3}$	rad/sec
Y_{PT}, $\dot{Y}_{PT}$	0	

Those initial conditions which were the same for all runs were:

Parameter	Value
ℓ_1, m_1, n_2, n_3	0
n_1	-1
p,q,r	0

Parameter	Value	
X_P, X_{P_T}	21.898824×10^6	ft
$\dot{X}_P$, $\dot{X}_{P_T}$, $\dot{Y}_P$, Z_{P_T}	0	
$\dot{Z}_P$, $\dot{Z}_{P_T}$	25,354.204	fps
θ_T	0	

Constants which were a function of spacecraft selection were:

Parameter	Value		
	Gemini	Agena	
D_{REF}	40	60	inches
d_{REF}	120	60	inches

Initial conditions which were a function of spacecraft selection and orientation were:

Parameter	Value		
	Gemini or Agena in orbital plane	Gemini normal	Agena normal
ℓ_2	0	+1	-1
ℓ_3	-1	0	0
m_2	-1	0	0
m_3	0	-1	+1
Y_P*	0	+	-
Z_P*	+	0	0

* The Y_P and Z_P magnitudes were varied as desired to provide the required initial LOS range.